ISSN: 1410-8917
Jurnal Kimia Sains & Aplikasi
e-ISSN: 2597-9914

Jurnal Kimia Sains dan Aplikasi 29 (3) (2026): 207-216

Jurnal Kimia Sains dan Aplikasi
Journal of Scientific and Applied Chemistry

Journal homepage: http://ejournal.undip.ac.id/index.php/ksa

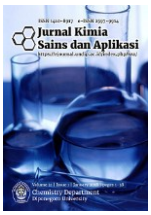

Biogenic Synthesis of TiO_2 Nanoparticles Mediated by the Ethanol Extract of Avocado Peel and Its Photocatalytic Activity on the Degradation of Rhodamine B

Devi Andalusia [1], Surya Lubis [2,*], Muliadi Ramli [2], Irfan Mustafa [2], Cantik Oriza Siregar [2]

[1] Master in Chemistry Program, Faculty of Mathematics and Natural Sciences, Universitas Syiah Kuala, Banda Aceh, Indonesia
[2] Department of Chemistry, Faculty of Mathematics and Natural Sciences, Universitas Syiah Kuala, Banda Aceh, Indonesia

* Corresponding author: suryalubis@usk.ac.id

https://doi.org/10.14710/jksa.29.3.207-216

Article Info

Article history:

Received: 08th November 2025
Revised: 25th February 2026
Accepted: 28th February 2026
Online: 22nd April 2026

Keywords:
TiO_2 NPs; Biogenic synthesis; Avocado peel; Photodegradation; Rhodamine B

Abstract

The synthesis of TiO_2 nanoparticles (TiO_2 NPs) using a green approach is highly preferred due to their non-toxicity and environmentally friendly nature. In this work, TiO_2 NPs were synthesized using titanium tetra-isopropoxide (TTIP) and ethanol extract of avocado peel (*Persea americana* Mill). The ethanol extract of avocado peel (EEAP) contained secondary metabolites, including phenolics, flavonoids, alkaloids, saponins, and terpenoids. These compounds play a role as a bioreductor to reduce metal ions, and as capping and stabilizing agents to control nanoparticle growth and prevent aggregation. The total phenolic content (TPC) of the EEAP was estimated using the Folin-Ciocalteu method, and the total flavonoid content (TFC) was evaluated using a colorimetric assay that involved aluminium chloride, and was 79.75 mg GAE/g and 21.74 mg QE/g, respectively. The characterization of as-synthesized TiO_2 NPs was carried out using Fourier Transform Infrared (FTIR) spectroscopy, X-ray powder diffraction (XRD), Scanning Electron Microscopy-Energy Dispersive X-Ray Spectroscopy (SEM-EDX), and UV-Vis Diffuse Reflectance Spectroscopy (UV-Vis DRS). The XRD patterns confirmed that the TiO_2 NPs were composed of anatase and rutile crystalline phases, with an average crystallite size of 19.27 nm. The TiO_2 NPs had a spherical shape with Ti, O, and C contents 84.9%, 10.24%, and 4.86%, respectively. The optical band gap of TiO_2 NPs was found to be 3.16 eV. The TiO_2 NPs were used as a photocatalyst for the degradation of rhodamine B (RhB) dye in a batch photoreactor. The TiO_2 NPs exhibited high photocatalytic activity in the degradation of RhB, with degradation percentages of up to 96.39% after 120 minutes of UV irradiation and 98.98% after 30 minutes of sunlight irradiation. The higher degradation percentage of RhB under sunlight than under UV irradiation can be attributed to the broad spectrum of sunlight and the dye-sensitization mechanism. Moreover, the results obtained confirmed that biogenically synthesized TiO_2 NPs offer a promising approach for removing organic pollutants and can be effectively utilized in wastewater treatment processes.

1. Introduction

The photocatalysis method has been used to degrade hazardous organic pollutants, such as dyes, into nontoxic compounds. Many types of semiconducting metal oxides can be used as photocatalysts, including ZnO, Fe_2O_3, SnO_2, and TiO_2. Particle size is an important factor influencing the photocatalytic activity of these materials. Semiconductor materials in nanoparticle size (1–100 nm) have a small particle size and large surface area that will positively impact their photocatalytic activity [1]. Titanium dioxide nanoparticles (TiO_2 NPs) are widely used as photocatalysts due to their characteristics, including availability, low cost, high thermal and

chemical stability, high photocatalytic activity, and oxygen vacancies in their lattice, which enhance photocatalytic efficiency [2, 3, 4].

Synthesis of nanoparticles can be carried out using biological methods, which are often referred to as green synthesis methods, which use bacteria, fungi, and plant extracts [5]. This method offers several advantages, including lower cost, higher efficiency, biocompatibility, relatively rapid processing, and environmental friendliness due to the minimal use of harmful chemicals [6]. Among these approaches, plant extract–mediated synthesis is the most widely used, as it does not require complex preparation, is faster, eliminates the need for culture maintenance, and is more cost-effective [7]. Nonetheless, this approach faces challenges, including poor reproducibility, non-uniformity of shape and particle size, complex extraction steps, low purity, scalability issues, and limited long-term stability. To overcome these drawbacks, researchers have focused on using sustainably available (non-seasonal) plants, using pure bioactive compounds instead of crude extracts, monitoring of synthesis parameters (e.g., pH, temperature, concentration of extract), simplifying extraction procedures, reducing energy consumption, and optimizing product yield and storage conditions [8, 9, 10].

Microbial synthesis also has several advantages, such as minimizing reliance on additional capping or stabilizing agents and enabling yield optimization through genetic modification. Furthermore, this method allows for rapid adjustments across diverse pathways, including extracellular, intracellular, and cell-free extract synthesis [11]. Microbial synthesis can produce nanoparticles with defined shape, size, composition, and particle monodispersity via the action of a specific enzyme [12]. Nevertheless, scaling up the process can be complicated by the requirements associated with microbial cultivation and preparation [13].

TiO_2 NPs have been synthesized using sweet lime (*Citrus limetta*) leaves extract [2], cinnamon powder extract [3] and red spinach (*Amaranthus tricolor L.*) [14]. The phytochemical content in plant extracts, such as phenolics, flavonoids, alkaloids, terpenoids, saponins, tannins, polysaccharides, and others, acts as bioreductors and stabilizers/capping agents in nanoparticle synthesis [15]. Flavonoids can be able to chelate and reduce metal ions into nanoparticles [16]. Flavonoids bind to titanium ions (Ti^{4+}) via their hydroxyl (-OH) and carbonyl (C=O) oxygen, forming a stable five- or six-membered ring structure [17]. Flavonoids also donate electrons to Ti^{4+} ions, reducing them to Ti^{3+} and forming nuclei that then grow into TiO_2 through a series of redox reactions involving oxygen from the surrounding environment [18].

Moreover, flavonoids also act as capping agents, stabilizing the TiO_2 nanoparticles and preventing aggregation, contributing to the uniform morphology of the synthesized nanoparticles. In parallel, phenolic compounds, characterized by hydroxyl-rich functional groups, contribute significantly to the reduction and stabilization of titanium ions. The hydroxyl groups interact with titanium ions, transferring electrons and aiding the controlled synthesis of nanoparticles with enhanced durability and functional properties [19]. Researchers have described a direct correlation between the total phenolic content and the metal-reducing capacity of the extracts and the NPs activities [20, 21]. Terpenoids also play a role in nanoparticle synthesis by reducing titanium ions and providing steric stabilization. The diversity of their structure enables them to interact with Titanium ions, influencing the morphology of TiO_2 NPs [19].

Herein, the use of avocado (*Persea americana* Mill) peel extract in the synthesis of TiO_2 NPs is reported. Avocado, a member of the Lauraceae family, is a fruit extensively cultivated in Indonesia, including in Aceh province. Avocado peels and seeds contain 21–30% of the total avocado fruit, which has the potential to be a waste, providing a sustainable and eco-friendly choice compared to other plant extracts. Avocado peels and seeds are reported to contain carbohydrates, proteins, lipids, fiber, and other active compounds such as flavonoids and phenolics in large quantities [22]. On the other hand, researcher was reported that the extract of avocado peel contains more flavonoids and phenolics compared to avocado seeds [23]. Avocado peel has the highest total phenolic and flavonoid contents among tropical fruit peels, including melon, passion fruit, banana, pineapple, watermelon, and papaya. Dried avocado peel had a total phenolic content of 4.3–120.3 mg GAE/g and showed the highest antioxidant activity (FRAP assay) compared with other fruit peels [24, 25]. The concentration and profile of phytochemicals in avocado peels vary and are influenced by factors such as maturity stage, cultivation conditions, and specific avocado varieties.

Additionally, the geographical origin, regional growth environment, and the selected extraction techniques play significant roles in determining these chemical properties [26]. The methanolic extract of avocado peel with a total phenolic content (TPC) of 21.833 $\pm$ 0.111 mg/100 g and a total flavonoid content (TFC) of 2.607 $\pm$ 0.111 mg/100 g had been reported [27]. The utilization of avocado peel extract in the synthesis of CdS NPs [28], Cu_2O NPs [29], and Ag NPs [30] had been reported. As far as we know, there is no report on the synthesis of TiO_2 NPs using the ethanol extract of avocado peel. The synthesized TiO_2 NPs in this study were applied to the photocatalytic degradation of RhB dye. RhB, a xanthene dyes are, dissolves easily in water and is usually utilized in the dying of cotton, bamboo, weed, and leather [31].

2. Experimental

2.1. Materials

All the chemicals utilized in this work were of analytical grade, except ethanol, which was 96% of technical grade. Titanium tetraisopropoxide (TTIP; 97%), Folin-Ciocalteu reagents, Mayer reagents, Wagner reagents, Dragendorff reagents, and Liebermann-Burchard reagents were bought from Sigma Aldrich St.

Louis USA, while RhB dye, gallic acid ($C_7H_6O_5$), Na_2CO_3, $AlCl_3$, methanol, potassium acetate (CH_3COOK), sodium chloride (NaCl), quercetin ($C_{15}H_{10}O_7$), Mg, HCl 37%, $FeCl_3.6H_2O$, were procured from Merck. The fresh avocado peels were taken from a juice seller in Banda Aceh, Indonesia.

2.2. Preparation of Avocado Peel Extract

The fresh avocado peels were cleaned using water to remove impurities, then rinsed using distilled water. The avocado peels were cut into small pieces and dried at room temperature for 3 days. Later, the dried avocado peels were crushed, and about 600 g of them were soaked in 1 L of 96% ethanol for 24 hours. After filtering the filtrate with Whatman filter paper, the extraction was repeated three times, changing the solvent to obtain the ethanol extract of avocado peel (EEAP). EEAP was employed for the synthesis of TiO_2 nanoparticles. The extracts were concentrated using a rotary evaporator for phytochemical screening and the determination of TPC and TFC.

2.3. Qualitative Phytochemical Screening

Phytochemical screening was conducted to determine the presence of secondary metabolites in the EEAP, such as phenolics, flavonoids, alkaloids, saponins, tannins, steroids, and terpenoids. The phytochemical screening was conducted using the standard phytochemical method [32, 33, 34]. The presence of alkaloids was detected using Mayer's reagent by the appearance of a cream-colored precipitate, Wagner's reagent by the appearance of a brown-red colored precipitate, and Dragendorff's reagent by the formation of a reddish-brown coloured precipitate. Detection of steroids and terpenoids was carried out by adding Liebermann Burchard reagent into EEAP. The presence of steroids was detected by the formation of a green color, while terpenoids were confirmed by the formation of a red color. Saponin detection was performed by mixing the EEAP with distilled water and boiling the mixture. The formation of a persistent froth for three minutes confirmed the presence of saponins. The existence of flavonoids was confirmed by the formation of pink or red color when Mg and HCl were added to the EEAP. The presence of phenolics was confirmed by the formation of a greenish-black or bluish-black color after the EEAP was added with $FeCl_3$.

2.4. Determination of TPC and TFC

The TPC was determined using gallic acid as a standard. 0.2 mL of EEAP at 20 mg/L was added to 15.8 mL of distilled water and 1 mL of Folin-Ciocalteu's reagent. After that, about 3 mL of 10% Na_2CO_3 was added to the mixture, which was then incubated for 2 hours at room temperature. The absorbance of the solution was determined using a Shimadzu UV 1900i UV-Vis spectrophotometer at 765 nm. The determination of TPC was carried out three times in repetition [23].

The TFC evaluation was conducted using quercetin as the standard. One mL of EEAP with a concentration of 20 mg/L was mixed with 3 mL of methanol, 0.2 mL of $AlCl_3$ solution, 0.2 mL of CH_3COOK 1 M, and 5.6 mL of distilled water. After incubation for about 30 minutes, the absorbance of the solution was measured using a Shimadzu UV-1900i UV-Vis spectrophotometer at 440 nm. The determination of TFC was carried out three times in repetition [35].

2.5. Synthesis of TiO_2 NPs

TiO_2 NPs were synthesized as previously reported with slight modifications [2]. A total of 11.45 mL of TTIP was added dropwise to 100 mL of distilled water while stirring. Furthermore, 50 mL of a 2 mg/mL EEAP solution was added dropwise to the above solution. The mixture was stirred continuously at 350 rpm for 3 hours, then filtered. The precipitate obtained was oven-dried at 100°C for 2 hours, and thereafter was calcined at 600°C for 3 hours in the muffle furnace. The selection of 600°C as the calcination temperature was based on its effectiveness in improving crystallinity, as reported for green tea-mediated synthesis of TiO_2 [36].

2.6. Characterization of TiO_2 NPs

TiO_2 NPs were characterized using X-ray Diffractometer (XRD, Shimadzu D6000 with Cu–kα radiation, λ = 0.154 cm^{-1}), operated at 40 kV, 15 mA, and scanning speed 10 minutes in the 2θ: 10°–90°. The surface shape and the presence of elements were characterized using a JEOL JSM-6510 LA Scanning Electron Microscope with Energy-Dispersive X-Ray Spectroscopy (SEM-EDX). The functional groups in the ethanol extract of avocado peel and the metal bonding were obtained using a Fourier Transform Infrared spectrophotometer (FTIR) with an IR Prestige-21 Shimadzu, over the range 400–4000 cm^{-1}. UV-Vis Diffuse Reflectance spectra were recorded using a Shimadzu UV-2450 UV-Vis spectrophotometer with a range of 200–800 nm.

2.7. Photocatalytic Degradation Experiments

The photocatalytic activity of TiO_2 NPs was studied on the removal of RhB dye. TiO_2 NPs (250 mg) and 25 mL of a 5 mg/L RhB solution at an initial pH of 5 were placed in a glass beaker and placed in the batch photoreactor. The solution was stirred magnetically at 250 rpm for 30 minutes in the dark, followed by 120 minutes of UV irradiation from a 6-watt UV lamp (λ = 254 nm). A sample was taken every 15 minutes, and the suspension was centrifuged at 4000 rpm for 15 minutes.

The absorbance of the supernatant was determined using a UV-Vis spectrophotometer (model UV-mini-1240 Shimadzu). The same procedure was performed using sunlight and without irradiation. The photocatalytic degradation experiments under sunlight irradiation were conducted outdoors at the Department of Chemistry, Faculty of Mathematics and Natural Sciences, Universitas Syiah Kuala, in August, during the time slot of 10:00 AM to 2:00 PM, under clear-sky conditions. The percentage of degradation of RhB was determined using Equation 1.

$$\%D = \frac{(A_0 - A_t)}{A_0} \times 100 \quad (1)$$

Where, A_o is the initial absorbance of RhB at λ_{max} of 553 nm, and A_t is the absorbance of RhB at λ_{max} of 553 nm at time *t*.

3. Results and Discussion

3.1. Qualitative Phytochemical Screening

The phytochemical screening is used to investigate the composition of the EEAP, which will play a role in the green synthesis of TiO_2 NPs. The qualitative phytochemical analysis is conducted as shown in Table 1. The EEAP contained alkaloids, flavonoids, terpenoids, saponins, and phenolics. Phytochemical screening results of the EEAP were almost similar to those previously reported [30, 37].

3.2. TPC and TFC

The TPC and TFC of the EEAP are 79.75 mg GAE/g and 21.74 mg QE/g, respectively. The results obtained in this study are in accordance with those reported in previous work, that avocado peel extract has a greater TPC than TFC [38]. Phenolic has a role in bioreductors and capping agents. Flavonoids are believed to be bioreductors that can chelate and reduce metal ions into nanoparticles [16]. It has been reported that the –OH groups' presence in phenolics and flavonoids played a role in the formation and stabilization of metal and metal oxide nanoparticles [14, 39].

Several studies have reported TPC values for plant extracts used in TiO_2 nanoparticle synthesis, including red spinach leaf extract (1.59 mg GAE/g), green tea extract (351.45 ± 7.546 mg AAE/100 g DW), and *Artemisia haussknechtii* (16.69 ± 1.73 mg GAE/g DW). In addition, TFC has been reported for green tea (12.425 ± 0.941 mg QE/g DW) and *Artemisia haussknechtii* (7.09 ± 1.22 mg RE/g DW) [14, 36, 40]. These findings indicate that EEAP exhibits strong potential as a sustainable reducing and stabilizing agent for TiO_2 nanoparticle synthesis.

3.3. Characteristics of the TiO_2 NPs

3.3.1. FTIR Analysis

FTIR spectroscopy was utilized to determine the chemical bonds and functional groups present in TiO_2 NPs. Figure 1 shows the FTIR spectrum of the EEAP, TiO_2 NPs before and after calcination. The spectrum of EEAP (Figure 1a) showed a broad peak at 3390 cm^{-1} ascribed to the stretching vibration of the hydroxyl (O-H) group, while the peak at 1610 cm^{-1} corresponded to the O-H bending vibration. The peaks at 2924 cm^{-1} and 2852 cm^{-1} are related to the symmetric and asymmetric stretching of C-H bonds [28]. The absorption band at 1722 cm^{-1} corresponded to the carbonyl C=O group; the peaks at 1443 and 1372 cm^{-1} were due to C-H bending, while the band at 1248 cm^{-1} was due to C-O [29]. Peaks at 1610 cm^{-1} and 1444 cm^{-1} could be related to C=C ring stretching. Figure 1b displays the FTIR spectrum of TiO_2 NPs before calcination. It can be observed that the intensities of the absorption bands at 3390, 2926, 2856, and 1610 cm^{-1} decrease, indicating the reduction of the titanium ion by secondary metabolites. FTIR spectrum of TiO_2 NPs before calcination also reveals a peak at 615 cm^{-1}, indicating the existence of Ti-O and O-Ti-O groups. This peak shifted to 503 cm^{-1} in the FTIR spectrum of TiO_2 NPs after calcination (Figure 1c). Moreover, the intensity of the absorption band at 3390 cm^{-1}, attributed to the O-H group, also decreases during calcination.

3.3.2. XRD Analysis

The determination of the phase, crystal structure, purity, and crystallite size of a material was analyzed by XRD. Figure 2 displays the diffraction peaks of TiO_2 NPs synthesized using EEAP. The peaks at 2θ values of 25.29°, 36.94°, 37.79°, 38.56°, 48.04°, 53.87°, 55.02°, 62.12°, 62.68°, 68.77°, 70.30°, 75.04°, 75.94°, 76.95°, and 80.70° attributed to the anatase phase in accordance with JCPDS Card 00-064-0863, while the peaks at 27.42°, 27.42°, 36.04°, 41.32°, and 56.55° are ascribed to rutile phase in accordance with JCPDS Card No. 01-086-0148. The most intense peak at 2θ of 25.29° indicates that TiO_2 NPs are predominantly oriented along the (101) plane [41]. The strong and sharp peaks of the XRD pattern in Figure 2 indicate the crystalline nature of TiO_2 NPs, which is reported to be more beneficial in regard to photocatalytic activity [42].

The relative percentages of the anatase and rutile phases were estimated by comparing the intensities of their characteristic XRD peaks according to Equations 2 [43] and 3 [44].

Table 1. Qualitative phytochemical screening of EEAP

Phytoconstituent	Name of Detection Test	Observation	Inference
Alkaloids	Mayer	Creamy white precipitate	+
	Dragendorff	Reddish-brown precipitate	+
Steroids	Liebermann	Yellow	–
Terpenoids	Liebermann	Red	+
Saponins	Frothing	Present froth	+
Flavonoids	Mg and HCl	Pink	+
Phenolics	$FeCl_3$	Dark green	+

(+): present; (–): absent

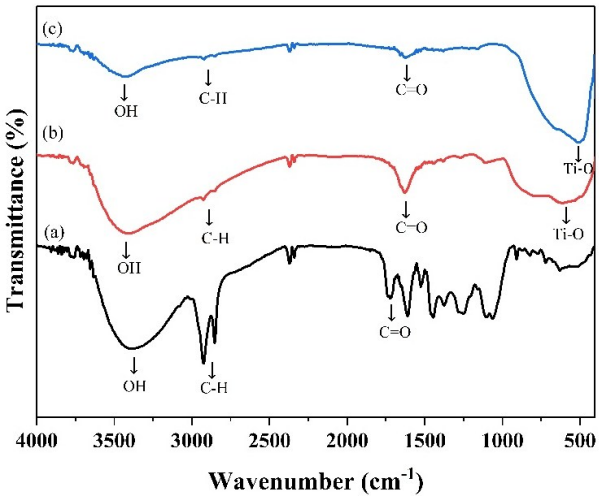

Figure 1. FTIR spectra of (a) ethanol extract of avocado peel, (b) TiO_2 NPs before calcination, and (c) TiO_2 NPs after calcination

$$f_A = \frac{1}{1+\frac{1}{K}\times\frac{I_R}{I_A}} \quad (2)$$

$$\%f_A = \frac{100 \times I_A}{I_A+\frac{1}{K}\times I_R} \quad (3)$$

Where, f_A represents the weight fraction of the anatase phase, I_R and I_A are X-ray diffraction intensities of anatase (101) and rutile (110) plane, respectively. The constant K is defined as 0.79 for $f_A > 0.2$ and 0.68 for $f_A \leq 0.2$. $\%f_A$ is the percentage weight of the anatase phase. Consequently, the rutile content is equal to $\%f_R = 100 - \%f_A$. Based on the above equation, the percentages of anatase and rutile phases in TiO_2 nanoparticles were determined to be 96.47% and 3.53%, respectively. The coexistence of anatase and rutile TiO_2 phases can enhance photocatalytic activity through the formation of a heterojunction. The mixed-phase TiO_2 with a small amount of rutile showed a higher photocatalytic activity by promoting efficient charge separation, where electrons migrate from the conduction band of rutile to anatase, while holes remain in rutile. This process suppresses electron–hole recombination, thereby improving the overall photocatalytic performance [43].

Based on XRD data results, the average crystallite size of the TiO_2 NPs was calculated by Debye-Scherrer's (Equation 4) [45].

$$D = \frac{K\lambda}{\beta \cos\theta} \quad (4)$$

Where, D is the crystallite size of the particle (nm), λ is the wavelength of the X-ray, k is the Scherrer constant (0.89), FWHM is the full-width at half maximum (FWHM) of the diffraction peak, and θ is the angle of the X-ray diffraction peak. The (101), (004), and (200) planes at 2θ of 25.29, 37.78, and 48.04° were selected to evaluate the crystallite size. The average crystallite size of the green synthesized TiO_2 NPs calculated by Equation 4 is approximately 19.27 nm. The average crystallite size of TiO_2 NPs synthesized in this study is smaller than that of TiO_2 NPs synthesized using the extract of *Citrus limetta* leaves [2] but larger than that of the TiO_2 NPs synthesized using the extract of red spinach leaves [14].

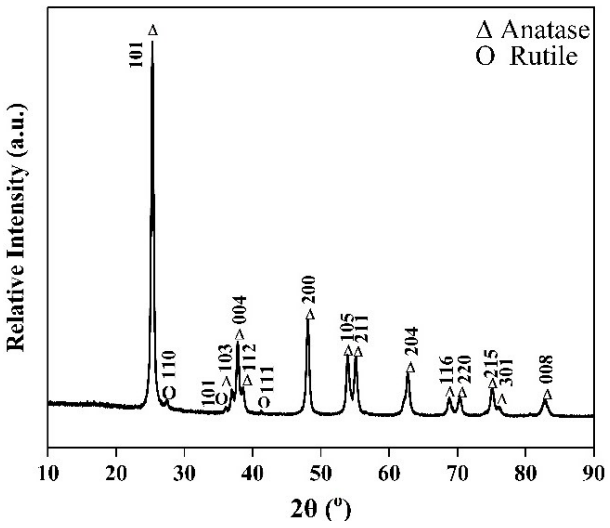

Figure 2. XRD patterns of TiO_2 NPs

3.3.3. SEM-EDX Analysis

The SEM image of TiO_2 NPs in Figure 3a indicates the formation of nanoparticles. It can be observed that the TiO_2 NPs are spherical and agglomerated. Spherical and agglomerated TiO_2 NPs synthesized by green synthesis have also been reported in previous studies [3, 6]. The particle size distribution shown in Figure 3b, determined using ImageJ software (n = 300 particles), indicates that TiO_2 NPs have a mean particle size of 90.35±0.82 nm. The nanoparticle size is larger than the crystallite size obtained from the Debye-Scherrer equation via XRD analysis. This difference in size is attributed to the agglomeration of TiO_2 NPs, which are formed by the clustering of several crystallites bound together [46]. Furthermore, the interactions and Van der Waals forces between the TiO_2 NPs significantly contribute to the formation of these agglomerates [47].

EDX was used to identify the elemental composition presence in TiO_2 NPs. The EDX spectrum (Figure 3c) revealed that Ti and O elements (84.90% and 10.24%) are dominant, which confirmed the formation of TiO_2 NPs. A small amount of carbon element (4.86%) was also observed in the EDX spectrum, which likely originated from residual secondary metabolites that remain on the TiO_2 NPs' surface after the calcination process. The presence of residual carbon on the TiO_2 NPs synthesized using Kinnow peel extract [48], *Lagenaria siceraria* leaf extract [41], and Fe_2O_3 NPs synthesized using aqueous extract of *Senegalia cathecu* [49] had also been reported. Carbon residue on the nanoparticle surface can act as a photosensitizer by broadening visible-light absorption and facilitating electron transfer to the conduction band of TiO_2 NPs. Furthermore, the electron will react with oxygen to generate a superoxide ion ($\cdot O^-_2$) that acts as a strong oxidant and enhances the photocatalytic activity of TiO_2 NPs. In addition, the residual carbon may alter the surface hydrophilicity of TiO_2 NPs, rendering them more hydrophobic and thereby decreasing their dispersion in water. Therefore, additional purification, such as ethanol washing, is required to minimize the residual carbon [48].

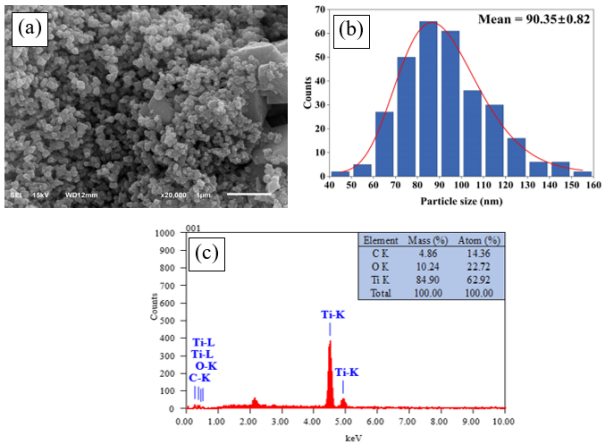

Figure 3. (a) SEM image of TiO_2 NPs, (b) particle size distribution histogram of TiO_2 NPs, and (c) EDX spectrum of TiO_2 NPs

3.3.4. UV-Vis DRS Analysis

The optical absorption bands of TiO_2 NPs synthesized using EEAP were characterized with UV-Vis DRS. Figure 4a shows the absorption spectrum of TiO_2 NPs in the range of 200–800 nm. TiO_2 NPs have a higher absorbance at a wavelength of 200–400 nm, which is the UV light region, and a weak absorbance in the visible light region, which is at a wavelength of 400-800 nm. Based on Figure 4b, the band gap energy of TiO_2 NPs using the Kubelka-Munk plot was calculated to be 3.16 eV. This finding indicated that the band gap energy of TiO_2 NPs synthesized using EEAP is lower than the reported value for pure anatase (3.2 eV). The reduction in band-gap energy relative to pure anatase may be attributed to the synergistic effects of the mixed anatase–rutile phase composition and the surface modification induced by the capping agent from the EEAP. XRD data revealed that TiO_2 NPs consist of 96.47% anatase and 3.53% rutile.

The existence of 3.53% of the rutile phase caused the reduction of the band gap energy of mixed-phase TiO_2 NPs. The heterojunction interface between the two TiO_2 polymorphs can induce interfacial strain and electronic coupling, thereby tuning the band-edge positions. The heterojunction between anatase and rutile facilitated efficient charge separation and suppressed electron-hole recombination, thereby enhancing overall photocatalytic activity [50]. On the other hand, the present carbon residue (as determined by EDX) from secondary metabolites in plant extracts might also contribute to reducing the band gap energy of TiO_2 NPs through carbon doping. Carbon might replace the oxygen site in the TiO_2 lattice. The surface-state modification also contributed to reducing the band gap energy of TiO_2 NPs, as functional groups such as –OH and –COOH from flavonoids and phenolics stabilized oxygen vacancies [51].

3.4. Photocatalytic Degradation of RhB

The photocatalytic activity of TiO_2 NPs was studied on the degradation of RhB under UV and sunlight irradiation. Figure 5 shows the absorbance spectra and the effect of time irradiation on the degradation of RhB dye under UV irradiation. The typical RhB absorbance peak at 553 nm decreased with increasing irradiation time. A decrease in the absorbance peak indicated a decrease in RhB concentration. Under dark conditions for 30 minutes, approximately 14.11% of RhB was removed by adsorption onto TiO_2 NPs.

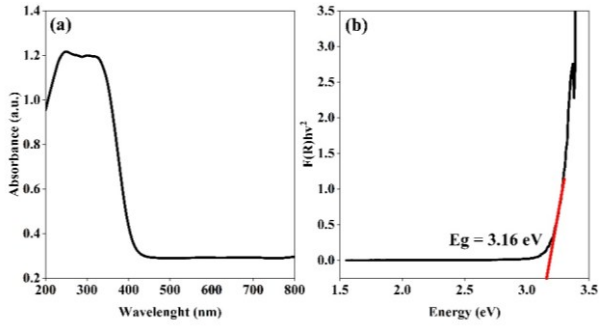

Figure 4. (a) Absorbance spectra and (b) Kubelka-Munk curve of the TiO_2 NPs

After irradiating the mixture with UV light for 15 minutes, the RhB concentration decreased by about 46.18%. The RhB dye removal increased to 96.38% after 120 minutes of irradiation. The enhancement of RhB dye degradation is attributed to the production of reactive species during the irradiation of TiO_2 NPs, such as hydroxyl radicals and holes, which oxidatively degrade RhB. The complete disappearance of the RhB absorption peak indicates that the RhB dye was fully photodegraded.

Figure 6 shows the degradation of RhB dye over TiO_2 NPs under different conditions and sources of light at regular intervals of time. It can be observed that sunlight irradiation produced much higher degradation efficiency of RhB than UV light. After 30 minutes of sunlight exposure, up to 98.98% of RhB was degraded, compared with 62.02% under UV light. Figure 6 also shows that the absorption percentage of RhB using TiO_2 NPs in the dark condition was 63.86% after 120 minutes, whereas under UV irradiation for 120 minutes, about 96.38% of RhB was removed. This observation confirmed the role of TiO_2 NPs in the photocatalytic degradation of RhB. When TiO_2 NPs are irradiated under UV or sunlight, electrons in the valence band (VB) are excited to the conduction band (CB), leaving holes (h^+) in VB. Electrons react with O_2 in reaction media to produce superoxide ion ($O_2^{-\bullet}$), while h^+ react with OH^- from H_2O to produce radical hydroxyl ($OH^\bullet$).

The superoxide ion and radical hydroxyl can degrade RhB. Several studies have reported that the degradation percentage of RhB dye over TiO_2 NPs obtained by green synthesis is in the range 80–96.59% after irradiating under UV light for 80–120 minutes [2, 52]. Figure 6 also showed that only 2.77% of RhB was removed after exposure to UV light (without TiO_2 NPs) for 120 minutes (photolysis). Based on these results, it is concluded that TiO_2 NPs synthesized using EEAP have high photocatalytic activity for the degradation of RhB dye under UV and sunlight irradiation.

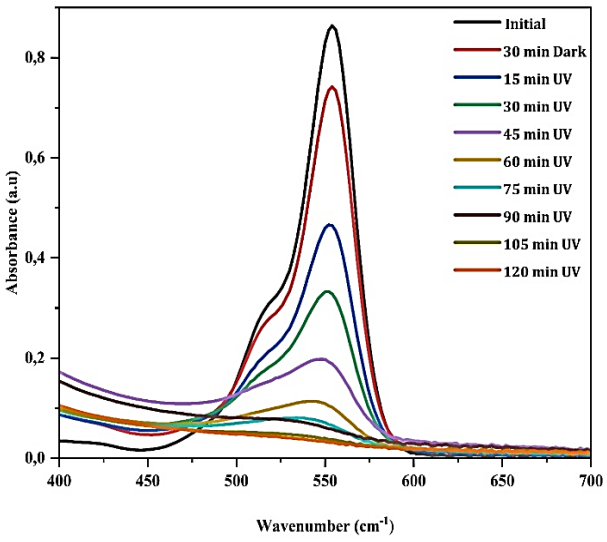

Figure 5. Absorbance spectra and the time reaction effect on the photodegradation of RhB dye using TiO_2 NPs under UV irradiation

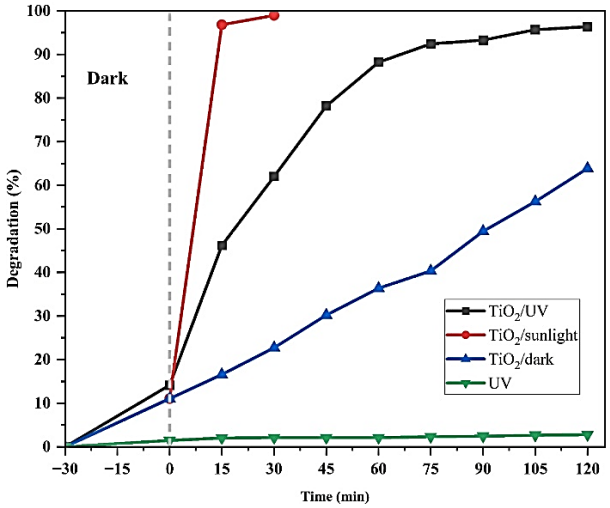

Figure 6. Degradation of RhB under dark conditions, photolysis, and photocatalysis

The higher degradation percentage of RhB using TiO_2 NPs observed under sunlight compared to UV irradiation can be ascribed to the broad spectrum of sunlight, which includes UV light (UVA (320–400 nm), UVB (290–320 nm), and UVC (< 290 nm)), visible light, and infrared [53], which activated the TiO_2 NPs more effectively than UV light (λ = 254 nm). The higher energy and intensity of photons in sunlight generate more electron-hole pairs, leading to increased production of hydroxyl radical (•OH) and superoxide ion radical ($^{-}$•O_2), which enhance the degradation efficiency of RhB dye. The increase in the photocatalytic activity of TiO_2 NPs can also be attributed to the dye-sensitization mechanism. RhB adsorbed on the surface of TiO_2 NPs is excited after absorbing visible light in sunlight, then an electron passes from its highest occupied molecular orbital (HOMO) to its lowest unoccupied molecular orbital (LUMO), and subsequently to the conduction band of TiO_2 NPs, thus triggering RhB degradation.

Along with RhB in solution, it can also absorb light, and the electron in the LUMO reacts with dissolved oxygen to produce the superoxide anion radical ($^{-}$•O_2) [54]. Moreover, the enhancement of the degradation percentage of RhB under sunlight irradiation was attributed to the heterojunction between mixed-phase TiO_2 NPs. The rutile phase has higher valence band and conduction band energies than the anatase phase. The photogenerated electrons will go to the anatase due to its lower conduction band minimum energy and react with oxygen to produce a superoxide ion, while holes will move to the rutile due to its higher valence band maximum energy and react with water to generate hydroxyl radicals [43].

4. Conclusion

TiO_2 NPs have been successfully synthesized using the ethanol extract of avocado peel and TTIP as a precursor. The EEAP contained alkaloids, flavonoids, terpenoids, saponins, and phenolics, which acted as bioreductor, stabilizer, and capping agent on the synthesis of TiO_2 NPs. The total phenolic and flavonoid content of the EEAP is 79.75 mg GAE/g and 21.74 mg QE/g. TiO_2 NPs synthesized using the EEAP were in anatase and rutile crystal phases, with an average crystallite size of 19.27 nm, spherical in shape, and slightly agglomerated. Particle size distribution of TiO_2 NPs ranged from 90 to 100 nm. The calculated band gap of TiO_2 NPs was 3.16 eV. TiO2 NPs showed high photocatalytic activity in degrading RhB under UV irradiation, with about 96.38% of the dye degraded within 120 minutes; under sunlight irradiation, about 98.98% of the dye was degraded within 30 minutes. The increase in photocatalytic activity of TiO_2 NPs under sunlight irradiation was attributed to the broad spectrum of sunlight, the dye-sensitization mechanism of RhB, and the heterojunction between rutile and anatase phases of the synthesized TiO_2 NPs. Based on the results, beyond RhB degradation, the biogenically synthesized TiO_2 NPs can be applied to remove other organic pollutants, such as pesticides, pharmaceutical residues, and textile dyes, as well as for water disinfection.

Acknowledgement

The authors gratefully acknowledge the Ministry of Education, Culture, Research and Technology, Republic of Indonesia, through Universitas Syiah Kuala, for funding this research under PFR Research Grant number 094/ES/PG.02.00.PL/2024.

References

[1] Danqi Li, Hongchen Song, Xia Meng, Tingting Shen, Jing Sun, Wenjia Han, Xikui Wang, Effects of Particle Size on the Structure and Photocatalytic Performance by Alkali-Treated TiO_2, *Nanomaterials*, 10, 3, (2020), 546 https://doi.org/10.3390/nano10030546

[2] Ghulam Nabi, Abdul Majid, Asma Riaz, Thamer Alharbi, Muhammad Arshad Kamran, Mansour Al-Habardi, Green synthesis of spherical TiO_2 nanoparticles using Citrus Limetta extract: Excellent photocatalytic water decontamination agent for RhB dye, *Inorganic Chemistry Communications*, 129, (2021), 108618 https://doi.org/10.1016/j.inoche.2021.108618

[3] Ghulam Nabi, Waseem Raza, M. B. Tahir, Green Synthesis of TiO_2 Nanoparticle Using Cinnamon Powder Extract and the Study of Optical Properties, *Journal of Inorganic and Organometallic Polymers and Materials*, 30, 4, (2020), 1425-1429 https://doi.org/10.1007/s10904-019-01248-3

[4] Nhung Thi-Tuyet Hoang, Anh Thi-Kim Tran, Thanh-An Le, D. Duc Nguyen, Enhancing efficiency and photocatalytic activity of TiO_2-SiO_2 by combination of glycerol for MO degradation in continuous reactor under solar irradiation, *Journal of Environmental Chemical Engineering*, 9, 5, (2021), 105789 https://doi.org/10.1016/j.jece.2021.105789

[5] Aymn Yaseen Sharaf Zeebaree, Samie Yaseen Sharaf Zeebaree, Rzgar Farooq Rashid, Osama Ismail Haji Zebari, Amal Jamil Sadiq Albarwry, Ardwan Fathi Ali, Ali Yaseen Sharaf Zebari, Sustainable engineering of plant-synthesized TiO_2 nanocatalysts: Diagnosis, properties and their photocatalytic performance in removing of methylene blue dye from effluent. A review, *Current Research in Green and Sustainable Chemistry*, 5, (2022), 100312 https://doi.org/10.1016/j.crgsc.2022.100312

[6] Diana Rakhmawaty Eddy, Devi Rahmawati, Muhamad Diki Permana, Takahiro Takei, Solihudin, Suryana, Atiek Rostika Noviyanti, Iman Rahayu, A review of recent developments in green synthesis of TiO_2 nanoparticles using plant extract: Synthesis, characterization and photocatalytic activity, *Inorganic Chemistry Communications*, 165, (2024), 112531 https://doi.org/10.1016/j.inoche.2024.112531

[7] Maria-Anna Gatou, Athanasia Syrrakou, Nefeli Lagopati, Evangelia A. Pavlatou, Photocatalytic TiO_2-Based Nanostructures as a Promising Material for Diverse Environmental Applications: A Review, *Reactions*, 5, (2024), 135-194 https://doi.org/10.3390/reactions5010007

[8] Shuaixuan Ying, Zhenru Guan, Polycarp C. Ofoegbu, Preston Clubb, Cyren Rico, Feng He, Jie Hong, Green synthesis of nanoparticles: Current developments and limitations, *Environmental Technology & Innovation*, 26, (2022), 102336 https://doi.org/10.1016/j.eti.2022.102336

[9] Kangkan Deka, Renaldy Donlang Nongbet, Karan Das, Pranjal Saikia, Simran Kaur, Abhijita Talukder, Bhargab Thakuria, Understanding the mechanism underlying the green synthesis of metallic nanoparticles using plant extract(s) with special reference to Silver, Gold, Copper and Zinc oxide nanoparticles, *Hybrid Advances*, 9, (2025), 100399 https://doi.org/10.1016/j.hybadv.2025.100399

[10] Anjuman Ayub, Atif Khurshid Wani, Suhaib Mohd Malik, Mehvish Ayub, Reena Singh, Chirag Chopra, Tabarak Malik, Green nanoscience for healthcare: Advancing biomedical innovation through eco-synthesized nanoparticle, *Biotechnology Reports*, 47, (2025), e00913 https://doi.org/10.1016/j.btre.2025.e00913

[11] Ahmed Ghareeb, Amr Fouda, Rania M. Kishk, Waleed M. El Kazzaz, Unlocking the potential of titanium dioxide nanoparticles: an insight into green synthesis, optimizations, characterizations, and multifunctional applications, *Microbial Cell Factories*, 23, 1, (2024), 341 https://doi.org/10.1186/s12934-024-02609-5

[12] Howra Bahrulolum, Saghi Nooraei, Nahid Javanshir, Hossein Tarrahimofrad, Vasighe Sadat Mirbagheri, Andrew J. Easton, Gholamreza Ahmadian, Green synthesis of metal nanoparticles using microorganisms and their application in the agrifood sector, *Journal of Nanobiotechnology*, 19, (2021), 86 https://doi.org/10.1186/s12951-021-00834-3

[13] Harjeet Singh, Martin F. Desimone, Shivani Pandya, Srushti Jasani, Noble George, Mohd Adnan, Abdu Aldarhami, Abdulrahman S. Bazaid, Suliman A. Alderhami, Revisiting the Green Synthesis of Nanoparticles: Uncovering Influences of Plant Extracts as Reducing Agents for Enhanced Synthesis Efficiency and Its Biomedical Applications, *International Journal of Nanomedicine*, 18, (2023), 4727-4750 https://doi.org/10.2147/IJN.S419369

[14] Devi Rahmawati, Muhamad Diki Permana, Diana Rakhmawaty Eddy, Norio Saito, Takahiro Takei, Suryana, Atiek Rostika Noviyanti, Iman Rahayu, Mohamed H. Helal, Zeinhom M. El-Bahy, Synthesis of TiO_2 nanoparticles using red spinach leaf extract (*Amaranthus Tricolor* L.) for photocatalytic of methylene blue degradation, *Green Chemistry Letters and Reviews*, 17, 1, (2024), 2352571 https://doi.org/10.1080/17518253.2024.2352571

[15] Sunita Patil, Rajkuberan Chandrasekaran, Biogenic nanoparticles: A comprehensive perspective in synthesis, characterization, application and its challenges, *Journal of Genetic Engineering and Biotechnology*, 18, 1, (2020), 67 https://doi.org/10.1186/s43141-020-00081-3

[16] Mohammad Aslam, Ahmad Zuhairi Abdullah, Mohd Rafatullah, Recent development in the green synthesis of titanium dioxide nanoparticles using plant-based biomolecules for environmental and antimicrobial applications, *Journal of Industrial and Engineering Chemistry*, 98, (2021), 1-16 https://doi.org/10.1016/j.jiec.2021.04.010

[17] Gregory Marslin, Karthik Siram, Qaisar Maqbool, Rajendran Kamalabai Selvakesavan, Dariusz Kruszka, Piotr Kachlicki, Gregory Franklin, Secondary Metabolites in the green synthesis of metallic nanoparticles, *Materials*, 11, 6, (2018), 940 https://doi.org/10.3390/ma11060940

[18] Ravi Saini, Pradeep Kumar, Green synthesis of TiO_2 nanoparticles using *Tinospora cordifolia* plant extract & its potential application for photocatalysis and antibacterial activity, *Inorganic Chemistry Communications*, 156, (2023), 111221 https://doi.org/10.1016/j.inoche.2023.111221

[19] Great Iruoghene Edo, Alice Njolke Mafe, Ali B. M. Ali, Patrick Othuke Akpoghelie, Emad Yousif, Endurance Fegor Isoje, Ufuoma Augustina Igbuku, Khalid Zainulabdeen, Joseph Oghenewogaga Owheruo, Arthur Efeoghene Athan Essaghah, Huzaifa Umar, Dina S. Ahmed, Ahmed A. Alamiery, Eco-friendly nanoparticle phytosynthesis via plant extracts: Mechanistic insights, recent advances, and multifaceted uses, *Nano TransMed*, 4, (2025), 100080 https://doi.org/10.1016/j.ntm.2025.100080

[20] Pablo Salgado, Katherine Márquez, Olga Rubilar, David Contreras, Gladys Vidal, The effect of phenolic compounds on the green synthesis of iron nanoparticles (Fe_xO_y-NPs) with photocatalytic activity, *Applied Nanoscience*, 9, 3, (2019), 371-385 https://doi.org/10.1007/s13204-018-0931-5

[21] Jian-Ai Quek, Jin-Chung Sin, Sze-Mun Lam, Abdul Rahman Mohamed, HongHu Zeng, Bioinspired green synthesis of ZnO structures with enhanced visible light photocatalytic activity, *Journal of Materials Science: Materials in Electronics*, 31, 2, (2020), 1144-1158 https://doi.org/10.1007/s10854-019-02626-w

[22] Clinton O. Nyakang'i, Rebecca Ebere, Eunice Marete, Joshua M. Arimi, Avocado production in Kenya in relation to the world, Avocado by-products (seeds and peels) functionality and utilization in food products, *Applied Food Research*, 3, 1, (2023), 100275 https://doi.org/10.1016/j.afres.2023.100275

[23] Mariel Calderón-Oliver, Héctor B. Escalona-Buendía, Omar N. Medina-Campos, José Pedraza-Chaverri, Ruth Pedroza-Islas, Edith Ponce-Alquicira, Optimization of the antioxidant and antimicrobial response of the combined effect of nisin and avocado byproducts, *LWT*, 65, (2016), 46-52 https://doi.org/10.1016/j.lwt.2015.07.048

[24] Sadiye Akan, Phytochemicals in avocado peel and their potential uses, *Food and Health*, 7, 2, (2021), 138-149 https://doi.org/10.3153/FH21015

[25] Damila R. Morais, Eliza M. Rotta, Sheisa C. Sargi, Eduardo M. Schmidt, Elton Guntendorfer Bonafe, Marcos N. Eberlin, Alexandra C. H. F. Sawaya, Jesuí V. Visentainer, Antioxidant activity, phenolics and UPLCESI(-)-MS of extracts from different tropical fruits parts and processed peels, *Food Research International*, 77, 3, (2015), 392-399 https://doi.org/10.1016/j.foodres.2015.08.036

[26] Morenikeji Abel Oke, Elijah Adegoke Adebayo, Nathaniel Aanu Ajisope, Busayo Mutiat Olowe, Oluwabunmi Susan Fasuan, Avocado (*Persea americana*) peel: a promising source of bioactive compounds, *Frontiers in Nutrition*, 12, (2025), 1642969 https://doi.org/10.3389/fnut.2025.1642969

[27] Nurdin Rahman, Sri Mulyani Sabang, Rukman Abdullah, Bohari Bohari, Antioxidant properties of the methanolic extract of avocado fruit peel (*Persea americana* Mill.) from Indonesia, *Journal of Advanced Pharmaceutical Technology & Research*, 13, 3, (2022), 166-170 https://doi.org/10.4103/japtr.japtr_22_22

[28] Zainab T. Turki, Aula M. Al Hindawi, Nagham M. Shiltagh, Green synthesis of CdS nanoparticles using avocado peel extract, *NanoWorld Journal*, 8, 3, (2022), 73-78 https://doi.org/10.17756/nwj.2022-102

[29] Fatih Özbaş, Sustainable Synthesis of Green Cu_2O Nanoparticles using Avocado Peel Extract as Biowaste Source, *Journal of the Turkish Chemical Society Section A: Chemistry*, 11, 1, (2024), 303-312 https://doi.org/10.18596/jotcsa.1391735

[30] Mohamed Yassin Ali, AboBaker Seddik Mahmoud, Mohnad Abdalla, Hamed I. Hamouda, Abeer S. Aloufi, Norah Saud Almubaddil, Yosra Modafer, Abdel-Moniem Sadek Hassan, Mostafa Abdel Makasoud Eissa, Daochen Zhu, Green synthesis of bio-mediated silver nanoparticles from *Persea americana* peels extract and evaluation of their biological activities: *In vitro* and *in silico* insights, *Journal of Saudi Chemical Society*, 28, 3, (2024), 101863 https://doi.org/10.1016/j.jscs.2024.101863

[31] Ashish V. Mohod, Malwina Momotko, Noor Samad Shah, Mateusz Marchel, Mohammad Imran, Lingshuai Kong, Grzegorz Boczkaj, Degradation of Rhodamine dyes by Advanced Oxidation Processes (AOPs)–Focus on cavitation and photocatalysis-A critical review, *Water Resources and Industry*, 30, (2023), 100220 https://doi.org/10.1016/j.wri.2023.100220

[32] J. B. Harborne, *Phytochemical Methods A Guide to Modern Techniques of Plant Analysis*, Chapman Hall, London, 1998,

[33] Junaid R. Shaikh, M. K. Patil, Qualitative tests for preliminary phytochemical screening: An overview, *International Journal of Chemical Studies*, 8, 2, (2020), 603-608 https://doi.org/10.22271/chemi.2020.v8.i2i.8834

[34] Muhammad Adil, Faten Zubair Filimban, Ambrin, Atifa Quddoos, Ayaz Ali Sher, Muhammad Naseer, Phytochemical screening, HPLC analysis, antimicrobial and antioxidant effect of *Euphorbia parviflora* L. (Euphorbiaceae Juss.), *Scientific Reports*, 14, 1, (2024), 5627 https://doi.org/10.1038/s41598-024-55905-w

[35] Aline Lamien-Meda, Charles Euloge Lamien, Moussa M. Y. Compaoré, Roland T. Meda, Martin Kiendrebeogo, Boukare Zeba, Jeanne F. Millogo, Odile G. Nacoulma, Polyphenol Content and Antioxidant Activity of Fourteen Wild Edible Fruits from Burkina Faso, *Molecules*, 13, 3, (2008), 581-594 https://doi.org/10.3390/molecules13030581

[36] Thi Kim Ngan Tran, Le Khanh Van Tran, Ngoc Cat Thuyen Vo, Ngoc Cat Nguyen Vo, Thi Que Minh Doan, Hoang Danh Pham, Thi Nhu Dung Nguyen, Green synthesis of titanium dioxide nanoparticles using green tea (*Camellia sinensis*) extract: Characteristics and applications, *Green Processing and Synthesis*, 14, 1, (2025), 20240226 https://doi.org/10.1515/gps-2024-0226

[37] Gelisa Wulandari, Asep Abdul Rahman, Rani Rubiyanti, Uji Aktivitas Antibakteri Ekstrak Etanol Kulit Buah Alpukat (*Persea americana* Mill) Terhadap Bakteri *Staphylococcus aureus*, *Media Informasi*, 15, 1, (2019), 74-80 https://doi.org/10.37160/bmi.v15i1.229

[38] Xiaoyan Lyu, Osman Tuncay Agar, Colin J. Barrow, Frank R. Dunshea, Hafiz A. R. Suleria, Phenolic Compounds Profiling and Their Antioxidant Capacity in the Peel, Pulp, and Seed of Australian Grown Avocado, *Antioxidants*, 12, 1, (2023), 185 https://doi.org/10.3390/antiox12010185

[39] Ahmed S. Abdelbaky, Taia A. Abd El-Mageed, Ahmad O. Babalghith, Samy Selim, Abir M. H. A. Mohamed, Green synthesis and characterization of ZnO nanoparticles using *Pelargonium odoratissimum* (L.) Aqueous Leaf Extract and Their Antioxidant, Antibacterial and Anti-inflammatory Activities, *Antioxidants*, 11, 8, (2022), 1444 https://doi.org/10.3390/antiox11081444

[40] Mehran Alavi, Naser Karimi, Characterization, antibacterial, total antioxidant, scavenging, reducing power and ion chelating activities of green synthesized silver, copper and titanium dioxide nanoparticles using *Artemisia haussknechtii* leaf extract, *Artificial Cells, Nanomedicine, and Biotechnology*, 46, 8, (2018), 2066-2081 https://doi.org/10.1080/21691401.2017.1408121

[41] Harpreet Kaur, Simerjeet Kaur, Sanjeev Kumar, Jagpreet Singh, Mohit Rawat, Eco-friendly Approach: Synthesis of Novel Green TiO_2 Nanoparticles for Degradation of Reactive Green 19 Dye and Replacement of Chemical Synthesized TiO_2, *Journal of Cluster Science*, 32, (2021), 1191-1204 https://doi.org/10.1007/s10876-020-01881-w

[42] Carol Langa, Zikhona N. Tetana, Nomso C. Hintsho-Mbita, Effect of calcination temperature on the synthesis of TiO_2 nanoparticles from *Sutherlandia frutescence* for the degradation of Congo red dye and antibiotics ciproflaxin and sulfamethoxazole, *Chemical Physics Impact*, 7, (2023), 100389 https://doi.org/10.1016/j.chphi.2023.100389

[43] Wei-Kang Wang, Jie-Jie Chen, Xing Zhang, Yu-Xi Huang, Wen-Wei Li, Han-Qing Yu, Self-induced synthesis of phase-junction TiO_2 with a tailored rutile to anatase ratio below phase transition temperature, *Scientific Reports*, 6, (2016), 20491 https://doi.org/10.1038/srep20491

[44] Ren Su, Ralf Bechstein, Lasse Sø, Ronnie T. Vang, Michael Sillassen, Björn Esbjörnsson, Anders Palmqvist, Flemming Besenbacher, How the Anatase-to-Rutile Ratio Influences the Photoreactivity of TiO_2, *The Journal of Physical Chemistry C*, 115, 49, (2011), 24287-24292 https://doi.org/10.1021/jp2086768

[45] P. Scherrer, Bestimmung der inneren Struktur und der Größe von Kolloidteilchen mittels Röntgenstrahlen, in: *Kolloidchemie Ein Lehrbuch*, Springer, Berlin, Heidelberg, 1912, https://doi.org/10.1007/978-3-662-33915-2_7

[46] Suci Wahyu Suciyati, Anisatul Mahmudah, Lusia Prastica, Ayu Aprilia, Biosynthesis of ZnO Nanoparticles from *Cnidoscolus aconitifolius* Leaf Extract: Structure, Morphology, and Photocatalytic Performance for Methylene Blue and Methyl Orange Degradation by UV Light Irradiation, *Jurnal Kimia Sains dan Aplikasi*, 28, 9, (2025), 502-511 https://doi.org/10.14710/jksa.28.9.502-511

[47] Mamo Dikamu Dilika, Gada Muleta Fanta, Tomasz Tański, Green Synthesis of Titanium Dioxide Nanoparticles Using *Maerua oblongifolia* Root Bark Extract: Photocatalytic Degradation and Antibacterial Activities, *Materials*, 17, 23, (2024), 5835 https://doi.org/10.3390/ma17235835

[48] Ajay Kumar Tiwari, Abhimanyu Kumar Singh, Saket Jha, Sharad Kumar Tripathi, Ram Raseele Awasthi, Sheo K. Mishra, Rudra Prakash Ojha, Abhishek Kumar Bhardwaj, Anupam Dikshit, Green synthesis of TiO_2 nanoparticles using Kinnow peel extracts and their antioxidant properties, *Scientific Report*, 15, (2025), 38307 https://doi.org/10.1038/s41598-025-22078-z

[49] Devendra Khadka, Prayas Gautam, Rabin Dahal, Moses D. Ashie, Hari Paudyal, Kedar Nath Ghimire, Bishweshwar Pant, Bhoj Raj Poudel, Bishnu Prasad Bastakoti, Megh Raj Pokhrel, Evaluating the Photocatalytic Activity of Green Synthesized Iron Oxide Nanoparticles, *Catalysts*, 14, 11, (2024), 751 https://doi.org/10.3390/catal14110751

[50] Diana Rakhmawaty Eddy, Muhamad Diki Permana, Lintang Kumoro Sakti, Geometry Amal Nur Sheha, Solihudin, Sahrul Hidayat, Takahiro Takei, Nobuhiro Kumada, Iman Rahayuada, Heterophase Polymorph of TiO_2 (Anatase, Rutile, Brookite, TiO_2 (B)) for Efficient Photocatalyst: Fabrication and Activity, *Nanomaterials*, 13, 4, (2023), 704 https://doi.org/10.3390/nano13040704

[51] Nasir Shakeel, Ireneusz Piwoński, Parvaz Iqbal, Aneta Kisielewska, Green Synthesis of Titanium Dioxide Nanoparticles: Physicochemical Characterization and Applications: A Review, *International Journal of Molecular Sciences*, 26, 12, (2025), 5454 https://doi.org/10.3390/ijms26125454

[52] Afzal Ansari, Vasi Uddin Siddiqui, Wahid Ul Rehman, Md Khursheed Akram, Weqar Ahmad Siddiqi, Abeer M. Alosaimi, Mahmoud A. Hussein, Mohd Rafatullah, Green Synthesis of TiO_2 Nanoparticles Using *Acorus calamus* Leaf Extract and Evaluating Its Photocatalytic and In Vitro Antimicrobial Activity, *Catalysts*, 12, 2, (2022), 181 https://doi.org/10.3390/catal12020181

[53] Hironobu Ikehata, Tetsuya Ono, The Mechanisms of UV Mutagenesis, *Journal of Radiation Research*, 52, 2, (2011), 115-125 https://doi.org/10.1269/jrr.10175

[54] Jennyfer Diaz-Angulo, Islen Gomez-Bonilla, Christian Jimenez-Tohapanta, Miguel Mueses, Maria Pinzon, Fiderman Machuca-Martinez, Visible-light activation of TiO_2 by dye-sensitization for degradation of pharmaceutical compounds, *Photochemical and Photobiological Sciences*, 18, (2019), 897-904 https://doi.org/10.1039/c8pp00270c